

H. Sone · Y. Kagawa

## Pancreatic beta cell senescence contributes to the pathogenesis of type 2 diabetes in high-fat diet-induced diabetic mice

Received: 23 February 2004 / Accepted: 9 August 2004 / Published online: 29 December 2004  
© Springer-Verlag 2004

**Abstract** *Aims/hypothesis:* During the pathogenesis of type 2 diabetes insulin resistance causes compensatory proliferation of beta cells. As beta cells have a limited replication potential, this compensatory proliferation might accelerate cellular senescence and lead to diabetes. We examined the cellular senescence of beta cells after proliferation during lipoglutotoxicity. *Methods:* Senescence-associated markers in beta cells were examined in nutrient-induced diabetic C57BL/6J mice that were fed a high-fat diet. After 4 and 12 months of the high-fat diet, intraperitoneal glucose tolerance tests (IPGTTs) and histochemical analyses of Ki-67, p38, senescence-associated beta-galactosidase, and beta cell mass were performed. *Results:* At 4 months, the AUC for plasma insulin levels during the IPGTT ( $AUC_{\text{insulin}}$ ) was higher, beta cell mass was 3.1-fold greater, and the proliferation of beta cells was 2.2-fold higher than in the control group. However, at 12 months,  $AUC_{\text{insulin}}$  declined, the frequency of Ki-67-positive beta cells decreased to one-third that of the control group, and the senescence-associated, beta-galactosidase-positive area increased to 4.7-fold that of the control group. Moreover, small amounts of p38, which is induced by oxidative stress and mediates cellular senescence, were found in beta cells from the high-fat diet group, but not in beta cells from the control group. Furthermore, the senescence-associated, beta-galactosidase-positive area in the high-fat diet group had a highly significant negative correlation with  $AUC_{\text{insulin}}$  ( $r=-0.852$ ,  $p<0.01$ ). *Conclusions/interpretation:* Beta cell senescence occurred in diet-induced type 2 diabetes and led to insufficient insulin release. These findings suggest that cellular se-

nescence contributes to the pathogenesis of diet-induced diabetes.

**Keywords** Cellular proliferation · Cellular senescence · High-fat diet · Pancreatic beta cell · Type 2 diabetes

**Abbreviations**  $AUC_{\text{glucose}}$ : AUC for plasma glucose levels during IPGTT ·  $AUC_{\text{insulin}}$ : AUC for plasma insulin levels during IPGTT · ERK: extracellular signal-regulated kinase · IPGTT: intraperitoneal glucose tolerance test · JNK: c-Jun N-terminal kinase · MAPK: mitogen-activated protein kinase · ROS: reactive oxygen species · SA beta-gal: senescence-associated beta-galactosidase · TUNEL: terminal deoxynucleotidyl transferase-mediated dUTP nick-end labelling

### Introduction

Defective insulin secretion in type 2 diabetes mellitus is caused by beta cell dysfunction and reduced beta cell mass. Beta cell dysfunction is caused by chronic hyperglycaemia and/or hyperlipidaemia respectively referred to as glucotoxicity and lipotoxicity, which have been previously reviewed in detail [1–3].

Long-term regulation of beta cell mass is determined by the balance of beta cell growth, including replication and neogenesis, and beta cell loss through apoptosis, necrosis and senescence [4–7]. Decreased beta cell mass occurs in humans with type 2 diabetes and animal models of type 2 diabetes [6–12]. Chronic hyperglycaemia leads to progressive loss of beta cell mass with a prolonged increase in the rate of beta cell apoptosis without a compensatory increase in beta cell growth. In addition to necrosis, markedly increased beta cell apoptosis is regarded as one of the major factors in the pathogenesis of diabetes. The cellular mechanisms of increased beta cell apoptosis, which include hyperglycaemia-induced oxidative stress [8, 12], are being intensively studied [13–18].

Beta cell senescence also affects beta cell mass, but has not been studied in diabetes. Mammalian cells, with the

H. Sone · Y. Kagawa (✉)  
High Technology Research Centre, Kagawa Nutrition  
University,  
3-9-21 Chiyoda,  
Sakado, 350-0288, Japan  
e-mail: kagawa@eiyo.ac.jp  
Tel.: +81-49-2843479

Y. Kagawa  
Department of Biochemistry, Jichi Medical School,  
Tochigi-ken, Japan

exceptions of germ line cells and stem cells, have a limited replication potential *in vivo*, defined as replicative senescence, which amounts to irreversible growth arrest after a limited number of cell divisions [19]. Cellular senescence is also associated with reactive oxygen species (ROS), the incessant damaging products generated from aerobic metabolism such as oxidative stress [20–23]. During the pathogenesis of type 2 diabetes, beta cell proliferation increases to compensate for the increased insulin demand caused by insulin resistance, and the generation of ROS is induced by hyperglycaemia [6–8, 12, 24]. It would seem that beta cell proliferation and/or ROS generation accelerate cellular senescence and lead to diabetes. Type 2 diabetes in C57BL/6J mice is provoked by a high-fat diet and is associated with obesity, hyperglycaemia and hyperinsulinaemia [25, 26], which induce beta cell proliferation and ROS production in beta cells. To test the hypothesis that cellular senescence occurs in beta cells and contributes to the pathogenesis of type 2 diabetes, we fed C57BL/6J mice a high-fat diet for 12 months and examined cellular proliferation and ageing markers in the beta cells.

## Materials and methods

**Animals** Six-week-old C57BL/6J male mice were purchased from Clea Japan (Tokyo, Japan). The control group was fed a normal diet (AIN-93; 14% protein, 72% carbohydrates, 4% fat) [27], with free access to water. The high-fat diet group was given free access to a high-fat diet, in which beef tallow replaced 36% of the carbohydrates in the normal diet (high-fat diet: 14% protein, 36% carbohydrates, 40% fat). The mice were housed in a temperature-controlled room with a 12 h light–dark cycle. All experiments were approved by the Animal Ethics Committee of Kagawa Nutrition University and complied with the “Principles of laboratory animal care” (NIH publication no. 85-23, revised 1985).

**Blood analysis and glucose tolerance tests** For the intraperitoneal glucose tolerance test (IPGTT), mice fasted for 12 h and blood was drawn from the tail vein at 0, 30, 60 and 120 min after *i.p.* injection of glucose (2 g/kg of body weight). To measure plasma lipids, blood was collected from the tail vein before the *i.p.* injection of glucose. Plasma glucose, NEFA, triglycerides and total cholesterol were measured by commercial kits (Wako Pure Chemical Industries, Osaka, Japan). Plasma insulin was measured using a rat insulin enzyme immunoassay system (Amersham Biosciences, Piscataway, NJ, USA). At each time point, blood samples (approximately 70  $\mu$ l) were taken in one capillary tube, with the exception of the blood samples taken at the 0 time point (approximately 100  $\mu$ l in 1.5 capillary tubes). Because of the small body weight of the mice, the blood volume needed for microanalyses was only 2  $\mu$ l, with the exception of the insulin analyses (20  $\mu$ l). The trapezoid rule was used to determine the AUC for glucose and insulin concentrations in each animal.

The insulinogenic index was calculated by dividing the AUC for plasma insulin levels during IPGTT ( $AUC_{\text{insulin}}$ ) by the AUC for plasma glucose levels during IPGTT ( $AUC_{\text{glucose}}$ ) (0–30 min).

**Isolation of islets and islet study** Islets were isolated from the pancreas by collagenase digestion and collected under a microscope after 4 and 12 months of the high-fat diet. Islets were cultured for 12 h in RPMI 1640 medium containing 11.1 mmol/l glucose, 10% heat-inactivated fetal bovine serum, 100 IU/ml penicillin and 100  $\mu$ g/ml streptomycin, as previously described [28, 29]. Then, size-matched islets were pre-incubated for 60 min at 37 °C with KRB containing 0.2% BSA and 2.8 mmol/l glucose. After pre-incubation, 10 islets were stimulated with KRB at the indicated concentration of glucose for 1 h at 37 °C. Immediately thereafter, the supernatant was collected and stored at –80 °C until the insulin assay. Then, islets were washed with PBS three times and homogenised with acid ethanol (0.18 mol/l HCl in 95% ethanol) to determine the insulin content.

**Immunohistochemical analysis** For double-immunohistochemical staining of insulin and glucagon, Ki-67, or phospho-p38 (Thr180/Tyr182), pancreases from mice after 4 and 12 months of the experimental period were weighed, fixed overnight in 4% paraformaldehyde at 4 °C, embedded in paraffin, and sectioned. Three sections (3  $\mu$ m) separated by 200  $\mu$ m were incubated with rabbit anti-human glucagon polyclonal antibody (DakoCytomation, Carpinteria, CA, USA) diluted to 1:100, rat anti-mouse Ki-67 monoclonal antibody (TEC-3; DakoCytomation) diluted to 1:50, or mouse anti-human phospho-p38 monoclonal antibody (28B10; New England BioLabs, Beverly, MA, USA) diluted to 1:50. As secondary antibodies, swine anti-rabbit IgG (DakoCytomation) diluted to 1:1,000, rabbit anti-rat IgG antibody (DakoCytomation) diluted to 1:200, or rabbit anti-mouse IgG antibody (Rockland, Gilbertsville, PA, USA) diluted to 1:1,000 were used. We used 3,3'-diaminobenzidine tetrahydrochloride (DAB; Dojin, Tokyo, Japan) as substrate chromogen. Next sections were washed with 0.1 mol/l glycine–HCl buffer (pH 2.2) following incubation with guinea pig anti-porcine insulin antibody (DakoCytomation) diluted to 1:200. As a secondary antibody, rabbit anti-guinea pig IgG coupled to peroxidase (Rockland) diluted to 1:1,000 was used. Sections were stained with 3-amino-9-ethylcarbazole (Sigma-Aldrich, St. Louis, MO, USA) as substrate chromogen and counterstained in haematoxylin.

**Pancreatic islet morphology** For morphometric analysis of beta cell mass, three sections of each pancreas were covered systematically by capturing images from non-overlapping fields with a digital camera (Nikon 950; Nikon, Tokyo, Japan). The islet area and the section area were analysed using NIH Image 1.63 software, as previously described [30]. The percentage of beta cell area in the islet area was calculated by dividing the area of all insulin-positive cells by the islet area and by multiplying

by 100. The islet mass was calculated by multiplying the pancreas weight by the percentage of islets per pancreas. The beta cell mass was calculated by multiplying islet mass by the percentage of beta cells per islet. To assess the relative rate of beta cell neogenesis from exocrine duct cells, we quantified the percentage of exocrine duct cells that were immunoreactive for insulin, as previously described [31]. The resulting data were expressed as the percentage of duct cells that were positive for insulin in each pancreas, and the mean was calculated for each group.

**Beta cell proliferation** Beta cell replication per islet was calculated by comparing the insulin and Ki-67 stains and averaging the number of Ki-67-positive beta cells from approximately 80 islets per mouse.

**Detection of cellular senescence** Cellular senescence was evaluated by immunohistochemistry with cellular senescence marker phospho-p38 and by senescence-associated beta-galactosidase (SA beta-gal) staining. The frequency of beta cell senescence determined by immunohistochemistry was calculated using the method described for cell replication. The detection of SA beta-gal was performed as previously described [32] with minor modifications. After 12 months of the experimental period, pancreases were fixed for 3 h in 4% paraformaldehyde at 4 °C, placed overnight in PBS (pH 7.2) containing 30% sucrose at 4 °C, embedded in Tissue-Tek OCT compound (Miles, Elkhart, IN, USA), frozen, and sectioned into 8 µm thick slices by a refrigerated microtome. SA beta-gal was detected by a senescence detection kit (BioVision, Mountain View, CA, USA) and counterstained with Kernechtrot. For each pancreas, the images of islets in two sections separated by 200 µm were captured with a digital camera (Nikon). The SA beta-gal-positive area in the islets and the islet area were analysed using NIH Image 1.63 software, as previously described [30]. The percentage of SA beta-gal-positive area was calculated by dividing the SA beta-gal-positive area in the islets by the islet area and multiplying by 100.

**Detection of apoptosis** To detect apoptosis, three sections (3 µm) separated by 200 µm were stained by the terminal deoxynucleotidyl transferase-mediated dUTP nick-end labelling (TUNEL) method using an in situ apoptosis detection kit (Wako Pure Chemical Industries, Japan). DAB was used as substrate chromogen. Frequency of pancreatic islet cell apoptosis, which was expressed as events per islet, was calculated by averaging the number of TUNEL-positive beta cells in approximately 60 islets from each pancreas.

**Statistical analysis** All data analyses were conducted using StatView 5.0 (SAS Institute, Cary, NC, USA). Data are shown as the mean ± SEM. Correlation analysis was performed between cellular senescence and cellular proliferation, AUC<sub>glucose</sub>, AUC<sub>insulin</sub>, insulinogenic index or p38 mitogen-activated protein kinase (MAPK). The significance of correlation coefficients was analysed by Fisher's *z*-transformation. Statistical analysis of the other data was performed with the Mann–Whitney *U*-test. We considered *p* values of less than 0.05 to be statistically significant.

## Results

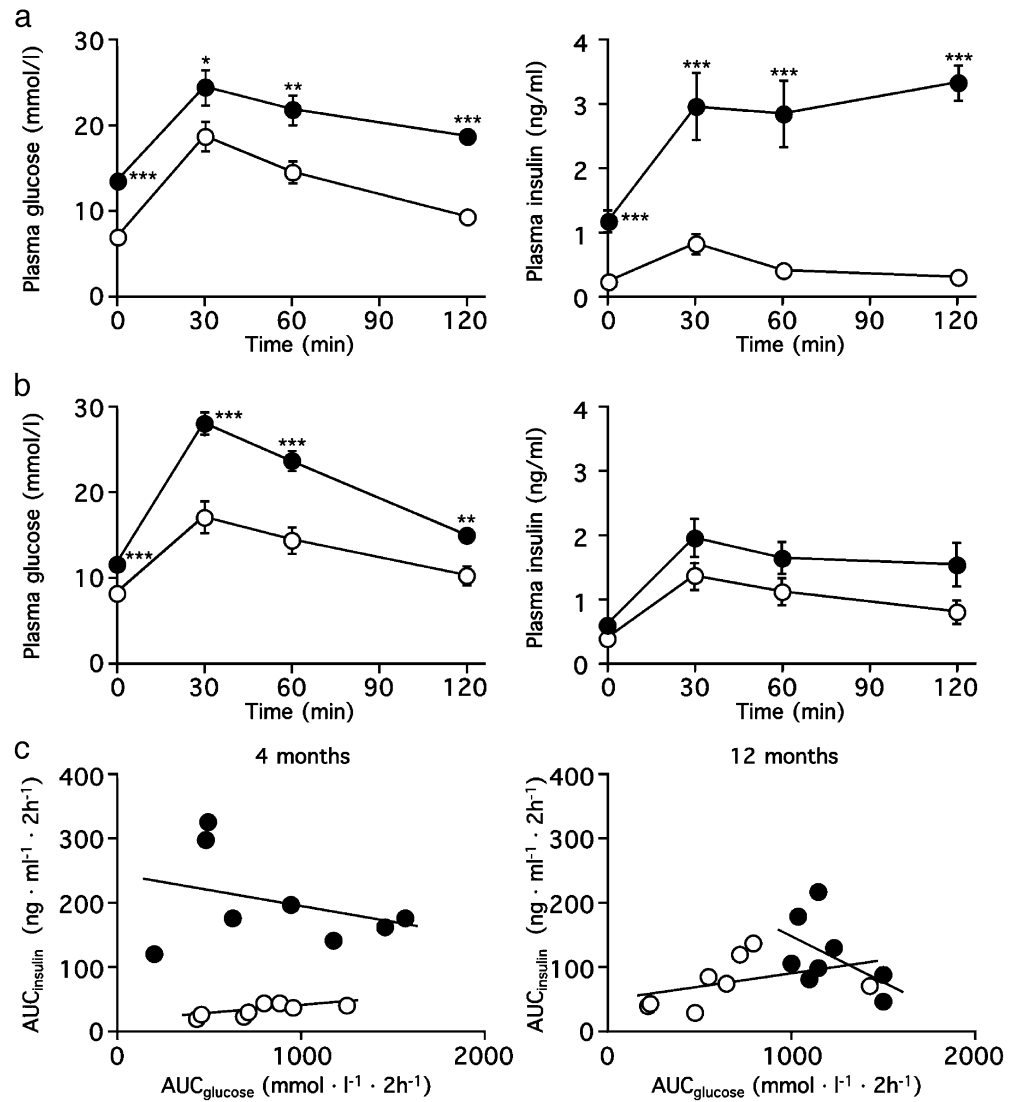
**Body weight, blood analyses, and glucose tolerance tests** Body weight, plasma glucose, insulin, NEFA, triglycerides, and total cholesterol measured after 4 and 12 months of the diet are shown in Table 1. Body weights were significantly higher in the high-fat diet group than in the control group after 4 and 12 months of the diet (*p*<0.001 and *p*<0.05, respectively). At 4 and 12 months, levels of plasma glucose and plasma lipids (NEFA, triglycerides, total cholesterol) were significantly higher in the high-fat diet group than in the control group (*p*<0.001). At 4 months, the insulin level of the high-fat diet group was increased to 5-fold that of the control group (*p*<0.001). However, at 12 months, the insulin level in the high-fat diet group did not differ from that in the control group, although the plasma glucose level remained high (*p*<0.001). In the mice fed a high-fat diet, weight loss was observed during the last 2 weeks of the 12-month

**Table 1** Body weight, plasma triglycerides, NEFA, total cholesterol, glucose, and insulin levels of C57BL/6J mice before and after 4 and 12 months of a high-fat diet

|                  | Body weight (g) | NEFA (mEq/l) | Triglycerides (mmol/l) | Total cholesterol (mmol/l) | Glucose (mmol/l) | Insulin (ng/ml) |
|------------------|-----------------|--------------|------------------------|----------------------------|------------------|-----------------|
| <i>0 months</i>  |                 |              |                        |                            |                  |                 |
| Control          | 21.7±0.3        | 0.56±0.03    | 1.05±0.04              | 3.0±0.04                   | 6.4±0.31         | 0.28±0.02       |
| High fat         | 22.0±0.2        | 0.57±0.03    | 1.02±0.05              | 2.9±0.07                   | 6.3±0.46         | 0.32±0.03       |
| <i>4 months</i>  |                 |              |                        |                            |                  |                 |
| Control          | 26.2±0.3        | 0.52±0.02    | 0.95±0.06              | 3.6±0.25                   | 6.9±0.16         | 0.24±0.05       |
| High fat         | 44.0±1.1***     | 0.88±0.06*** | 1.46±0.10***           | 6.2±0.55***                | 13.2±0.64***     | 1.20±0.20***    |
| <i>12 months</i> |                 |              |                        |                            |                  |                 |
| Control          | 30.5±0.6        | 0.61±0.05    | 0.84±0.02              | 2.5±0.07                   | 7.8±0.33         | 0.40±0.05       |
| High fat         | 40.4±3.8*       | 1.00±0.03*** | 1.48±0.06***           | 6.4±0.28***                | 11.6±0.35***     | 0.59±0.09       |

\**p*<0.05, \*\*\**p*<0.001 as compared with control (*n*=8)

**Fig. 1** Plasma glucose and plasma insulin levels in the IPGTT in C57BL/6J mice after 4 (a) and 12 (b) months of a control diet (open circles) and a high-fat diet (closed circles). c Correlations between  $AUC_{\text{glucose}}$  and  $AUC_{\text{insulin}}$  in the control group (open circles) and the high-fat diet group (closed circles) over 4 months (left) and 12 months (right). \*\*\* $p < 0.001$ , \*\* $p < 0.01$ , \* $p < 0.05$  as compared with the control group ( $n=8$ )



period. Ketoacidosis was hardly detected even after 12 months, despite the decreased body weight that alleviates insulin resistance (data not shown).

IPGTTs were performed after 4 and 12 months of the diet and evaluated by  $AUC_{\text{glucose}}$ ,  $AUC_{\text{insulin}}$ , and insulinogenic index (Fig. 1, Table 2). At 4 months, plasma glucose and insulin levels were significantly higher in the high-fat diet group than in the control group.  $AUC_{\text{insulin}}$  in the high-fat diet group was increased to 6.6-fold that of the control group ( $p < 0.001$ ). At 12 months,  $AUC_{\text{glucose}}$  was approximately 2-fold higher in the high-fat diet group than in the control group ( $p < 0.001$ ), but there was no difference in  $AUC_{\text{insulin}}$  between the two groups. In the high-fat diet group at 12 months, negative correlation ( $r = -0.509$ , not significant) was observed between  $AUC_{\text{insulin}}$  and  $AUC_{\text{glucose}}$  (the control group at 12 months:  $r = 0.425$ , not significant; the control and the high-fat diet groups at 4 months:  $r = 0.706$ ,  $p < 0.05$  and  $r = -0.234$ ,  $p =$  not significant, respectively). To access insulin release during IPGTT, the insulinogenic index was calculated (Table 2). Values of insulinogenic index ( $\text{ng}/\text{mmol}$ ) were  $53.5 \pm 5.8$

and  $220.6 \pm 63.0$  (control and high-fat diet groups at 4 months, respectively,  $p < 0.001$ ) and  $117.0 \pm 17.2$  and  $86.4 \pm 14.1$  (control and high-fat diet groups at 12 months, respectively, not significant). The insulinogenic index in the high-fat diet group at 12 months was lower than that of

**Table 2**  $AUC_{\text{glucose}}$ ,  $AUC_{\text{insulin}}$ , and insulinogenic index during IPGTT in C57BL/6J mice after 4 and 12 months of a high-fat diet

|  | 4 months               | 12 months              |
|--|------------------------|------------------------|
| $AUC_{\text{glucose}} (\text{mmol} \cdot \text{l}^{-1} \cdot 2 \text{h}^{-1})$ |                        |                        |
| Control  | $773.7 \pm 101.8$      | $623.4 \pm 145.0$      |
| High fat   | $870.9 \pm 188.0$      | $1140.9 \pm 62.9^{**}$ |
| $AUC_{\text{insulin}} (\text{ng} \cdot \text{ml}^{-1} \cdot 2 \text{h}^{-1})$  |                        |                        |
| Control  | $29.3 \pm 3.5$         | $73.8 \pm 14.6$        |
| High fat   | $193.9 \pm 30.5^{***}$ | $117.7 \pm 21.0$       |
| Insulinogenic index ( $\text{ng}/\text{mmol}$ )                                |                        |                        |
| Control  | $53.5 \pm 5.8$         | $117.0 \pm 17.2$       |
| High fat   | $220.6 \pm 63.0^{***}$ | $86.4 \pm 14.1$        |

\*\* $p < 0.01$ , \*\*\* $p < 0.001$  as compared with control ( $n=8$ )

control animals, although statistical significance was not attained. We also analysed insulin release during IPGTT (0–2 h) using  $AUC_{\text{insulin}}/AUC_{\text{glucose}}$ , and observed the same results as from the analysis using the insulinogenic index (data not shown). These results consolidate our suggestion of an impairment of insulin release in the high-fat diet group at 12 months. However, it is also possible that the reduced  $AUC_{\text{insulin}}$  during IPGTT may not indicate reduced beta cell function, but adjustment to reduced insulin resistance and reduced glycaemic load. Due to the limitations of this experiment, we could not further confirm these explanations.

**Islet studies** After 4 and 12 months of the diets, insulin release was stimulated with glucose in the static incubation experiments, and the insulin content in the islets was measured (Fig. 2). In the high-fat diet group at 4 months, the levels of insulin release induced by 16.7 and 33.4 mmol/l glucose ( $2.02 \pm 0.10$  and  $2.82 \pm 0.21$  ng islet<sup>-1</sup> h<sup>-1</sup>, respectively;  $p < 0.01$ ) were significantly higher than those in the control group ( $0.94 \pm 0.07$  and  $1.53 \pm 0.11$  ng islet<sup>-1</sup> h<sup>-1</sup>, respectively). However, at 12 months, the levels of insulin release in the high-fat diet group stimulated with 16.7 and 33.4 mmol/l glucose ( $0.76 \pm 0.13$  and  $1.13 \pm 0.25$  ng islet<sup>-1</sup> h<sup>-1</sup>, respectively) were almost the same as those in the control group ( $0.91 \pm 0.10$  and  $1.35 \pm 0.08$  ng islet<sup>-1</sup> h<sup>-1</sup>, respectively). Similarly, compared with the control group, the insulin content in islets of the high-fat diet group was significantly increased at 4 months ( $58.0 \pm 5.17$  and  $36.1 \pm 0.73$  ng/islet, respectively,  $p < 0.01$ ) and not different at 12 months ( $40.0 \pm 5.38$  and  $34.8 \pm 6.82$  ng/islet, respectively).

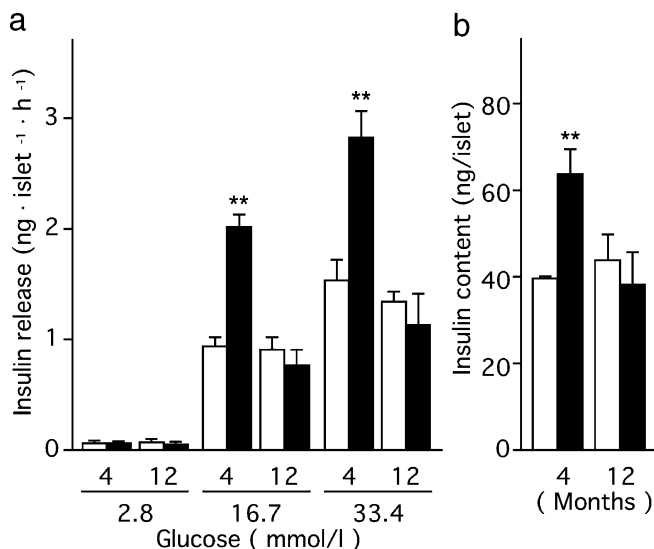


**Fig. 2** **a** Insulin release during static incubation with islets stimulated with 2.8, 16.7 or 33.4 mmol/l glucose over 4 and 12 months for each concentration. **b** Insulin content in islets of C57BL/6J mice after 4 and 12 months. *Open columns* control diet; *black columns* high-fat diet. \*\* $p < 0.01$  as compared with the control group ( $n = 6$ )

**Beta cell mass and proliferation** Morphometric analyses of beta cell mass and proliferation were performed by immunohistochemical analysis at 4 and 12 months. After 4 months, the islet area in the pancreases of the high-fat diet group was 2.2-fold larger than that in the control group, and the relative distribution of beta cells in the islets was slightly but significantly increased compared with that in the control group ( $p < 0.001$  and  $p < 0.05$ , respectively; Table 3). Moreover, the islet mass and the beta cell mass in the high-fat diet group were increased to 2.8-fold and 3.1-fold of that in the control group ( $p < 0.001$ ; Table 3). However, at 12 months, the significant differences in beta cell area, islet area, and pancreas weight between the two groups had disappeared. In the high-fat diet group at 4 and 12 months, newly formed duct-associated islet-like beta cell clusters that indicate beta cell neogenesis were identified (Fig. 3g, h). There was an increased percentage of beta cell neogenesis in duct cells from the high-fat diet group when compared with the control group at both 4 ( $0.78 \pm 0.03\%$  vs.  $0.31 \pm 0.02\%$  insulin-positive duct cells,  $p < 0.05$ ) and 12 months ( $0.80 \pm 0.06\%$  vs.  $0.38 \pm 0.03\%$  insulin-positive duct cells,  $p < 0.05$ ). But, there was no difference between the percentages of beta cell neogenesis in the high-fat group at 4 and 12 months.

At 4 months, the proliferation of beta cells (evaluated by the frequency of Ki-67-positive beta cells/islet) in the high-fat diet group was 2.2-fold higher than that of the control group to compensate for the increased insulin demand ( $p < 0.01$ ; Fig. 4). However, at 12 months, the frequency of Ki-67-positive beta cells in the high-fat diet group was decreased to one-third of that in the control group ( $p < 0.001$ ), while the number of beta cells undergoing replication in the control group was also reduced with ageing ( $p < 0.05$ ).

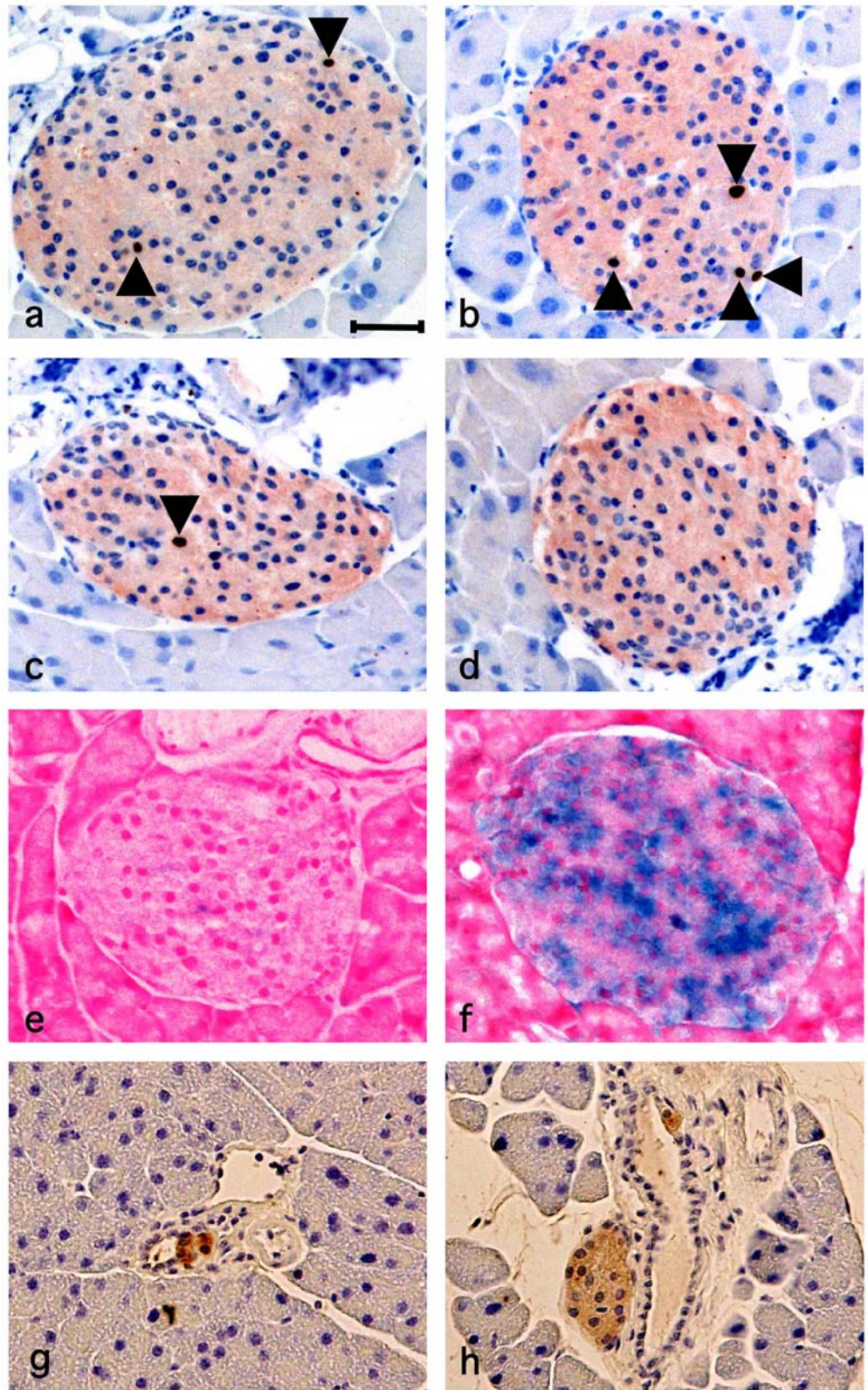
**Beta cell senescence and apoptosis** Cellular senescence and apoptosis in islets were evaluated after 12 months of the high-fat diet (Fig. 5). The percentage of SA beta-gal-positive area in islets from the high-fat diet group was

**Table 3** Morphometric analysis of pancreas of C57BL/6J mice after 4 and 12 months of a high-fat diet

|                            | Control          | High fat diet      |
|----------------------------|------------------|--------------------|
| <b>4 months</b>            |                  |                    |
| % Beta cell/islet          | 74.38 $\pm$ 2.10 | 80.52 $\pm$ 1.30*  |
| % Islet area/pancreas area | 0.91 $\pm$ 0.07  | 1.97 $\pm$ 0.07*** |
| Pancreas weight (g)        | 0.12 $\pm$ 0.01  | 0.16 $\pm$ 0.01**  |
| Islet mass (mg)            | 1.08 $\pm$ 0.13  | 3.07 $\pm$ 0.23*** |
| Beta cell mass (mg)        | 0.80 $\pm$ 0.10  | 2.47 $\pm$ 0.10*** |
| <b>12 months</b>           |                  |                    |
| % Beta cell/islet          | 76.40 $\pm$ 2.43 | 69.52 $\pm$ 3.40   |
| % Islet area/pancreas area | 1.37 $\pm$ 0.11  | 1.28 $\pm$ 0.40    |
| Pancreas weight (g)        | 0.13 $\pm$ 0.00  | 0.13 $\pm$ 0.00    |
| Islet mass (mg)            | 1.79 $\pm$ 0.16  | 1.55 $\pm$ 0.34    |
| Beta cell mass (mg)        | 1.37 $\pm$ 0.16  | 1.09 $\pm$ 0.28    |

\* $p < 0.05$ , \*\* $p < 0.01$ , \*\*\* $p < 0.001$  as compared with control ( $n = 4$ )

**Fig. 3** Double staining of Ki-67 protein (*brown*) and insulin (*pale red*) in islets of paraffin-embedded sections from C57BL/6J mice after 4 and 12 months of a control diet (**a, c**) and a high-fat diet (**b, d**). SA beta-gal staining in islets of frozen sections from C57BL/6J mice after 12 months of a control diet (**e**) and a high-fat diet (**f**). Insulin-stained, duct-associated beta cells from C57BL/6J mice after 4 (**g**) and 12 (**h**) months of a high-fat diet. Original magnification  $\times 300$  (*bar*=40  $\mu\text{m}$ )



4.7-fold that of the control group ( $12.4 \pm 3.7\%$  and  $2.4 \pm 0.4\%$  of islet area, respectively,  $p < 0.01$ ). In one mouse with aggravated high-fat diet-induced diabetes, senescent cells occupied 26% of the islet area (data not shown).

Phospho-p38 was slightly observed in the islets of the high-fat diet group ( $0.065 \pm 0.043$  phospho-p38-positive beta cells/islet), but not in the control group. There were 0.214 phospho-p38-positive beta cells/islet in the mouse

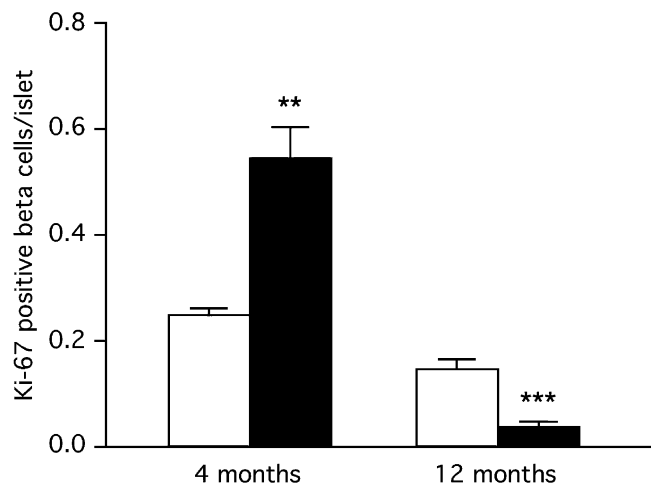


**Fig. 4** Frequency of beta cell proliferation evaluated by the number of Ki-67-positive beta cells in the islets of C57BL/6J mice after 4 and 12 months of a control diet (*open columns*) and a high-fat diet (*black columns*). \*\*\* $p < 0.001$ , \*\* $p < 0.01$  as compared with the control group ( $n = 5$ )

with aggravated high-fat diet-induced diabetes. The frequency of pancreatic islet cell apoptosis in the high-fat diet group was 4.6-fold that of the control group ( $1.44 \pm 0.20$  and  $0.31 \pm 0.02$  TUNEL-positive cells/islet, respectively,  $p < 0.01$ ).

*Correlation between cellular senescence and proliferation,  $AUC_{glucose}$ ,  $AUC_{insulin}$ , insulinogenic index and p38 MAPK* As shown in Fig. 6, the percentage of SA beta-gal-positive area was significantly correlated with Ki-67-positive beta cells and  $AUC_{glucose}$  ( $r = -0.864$ ,  $p < 0.001$  and  $r = 0.806$ ,  $p < 0.005$ , respectively). Moreover, in the high-fat diet group, the percentage of SA beta-gal-positive area had a significant negative correlation with  $AUC_{insulin}$

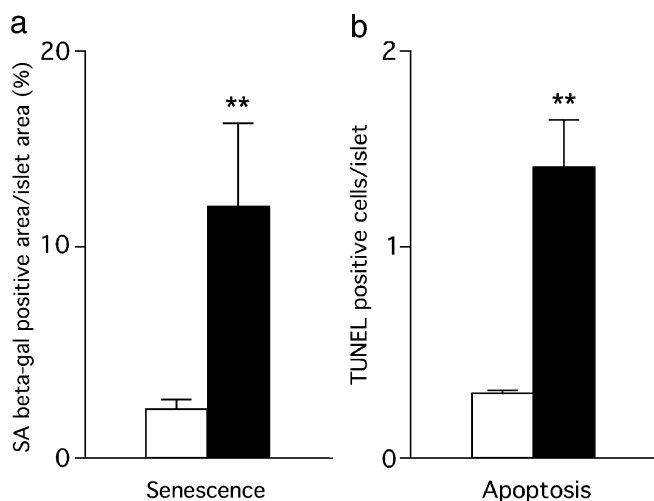


**Fig. 5** Percentage of senescent islet cells evaluated by SA beta-gal-positive area/islet area (a) and the frequency of apoptotic islet cells (b) evaluated by the number of TUNEL-positive cells in the islets of C57BL/6J mice after 12 months. *Open columns* control diet; *black columns* high-fat diet. \*\* $p < 0.01$  as compared with the control group ( $n = 5$ )

( $r = -0.852$ ,  $p < 0.01$ ), insulinogenic index ( $r = -0.857$ ,  $p < 0.05$ ), and a significant positive correlation with phospho-p38-positive beta cells ( $r = 0.843$ ,  $p < 0.05$ ). These results suggest that beta cell senescence may be induced through the p38 MAPK pathway and leads to reduced beta cell proliferation and insulin release.

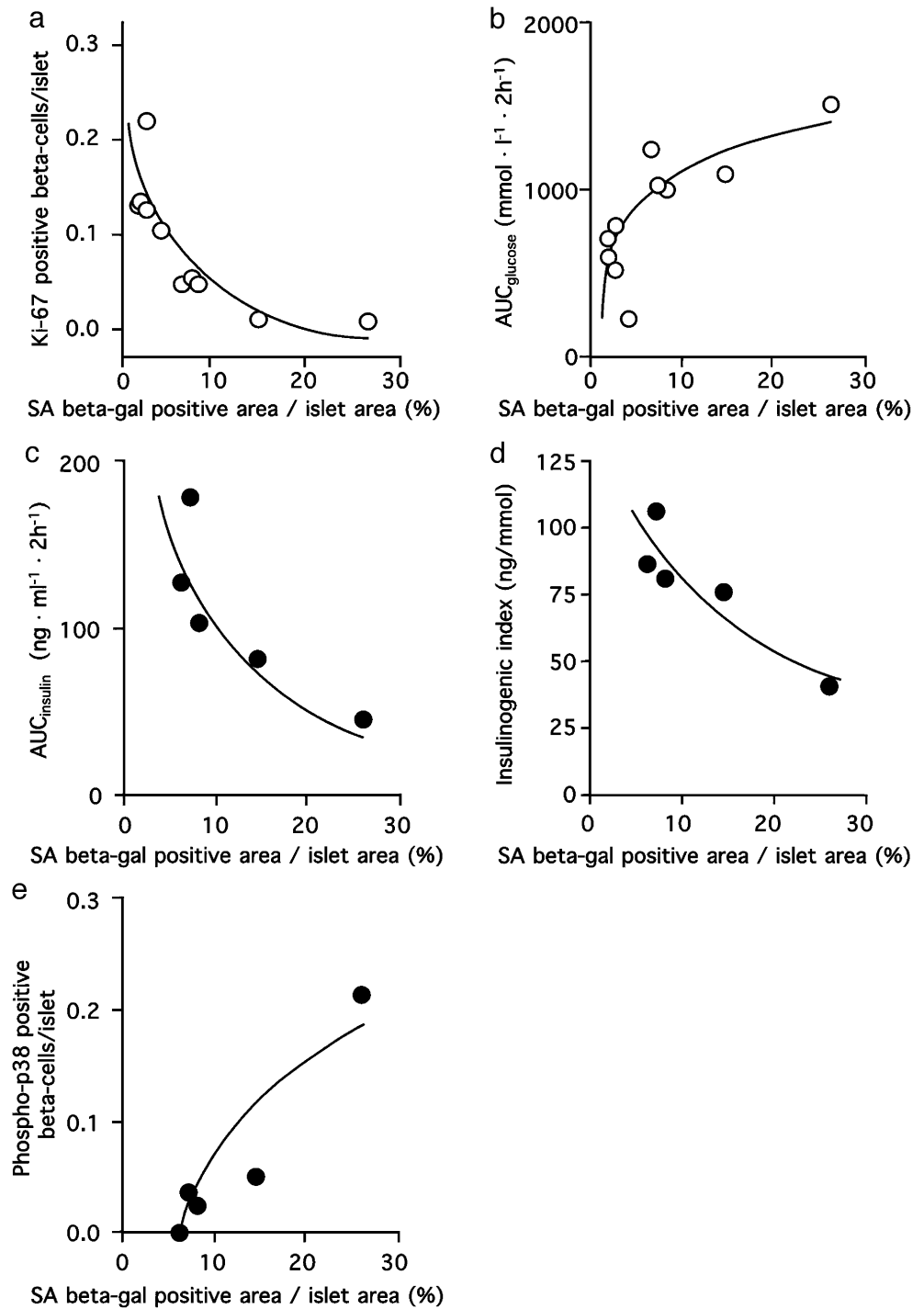
## Discussion

The markers of cellular senescence in beta cells were increased in mice fed a high-fat diet. Preceding senescence of the beta cells, increased proliferation was observed under hyperglycaemic conditions. There was a highly negative correlation between cellular proliferation and senescence. These findings indicate that cellular senescence occurs after rapid proliferation of beta cells and causes decreased cellular proliferation and beta cell mass.

Reduced pancreatic beta cell mass is a major factor in the pathogenesis of type 2 diabetes, as well as beta cell dysfunction. The long-term regulation of beta cell mass depends on the balance of beta cell supply from replication and neogenesis and beta cell death mainly from apoptosis [4–7]. To adapt to hyperglycaemia during the pathogenesis of type 2 diabetes, augmented beta cell proliferation causes a compensatory increase in beta cell mass. The disruption of an adequate increase in beta cell mass leads to type 2 diabetes [6–12]. After a long-term, high-fat diet, the beta cell proliferation markedly decreased and islet cellular senescence was observed. We were unable to perform beta-galactosidase staining on the islets from 4-month-old mice. However, if senescence stops proliferation, then the necrosis and apoptosis that follow will reduce islet mass. Cell division and cell death are independent events as in the case of neurons, but beta cells are vulnerable to lipoglutotoxicity, and islet mass may be decreased by apoptosis. Reduced hypertrophy may also contribute to the reduction of islet mass. To judge from these findings, beta cell senescence causes decreased beta cell mass and may lead to type 2 diabetes.

Cellular senescence and decreased cellular proliferation occur in chronic diseases with high cellular turnover. For example, liver cirrhosis, in which chronic hepatocyte death and renewal is the major predisposing factor, is caused by hepatocyte senescence with concomitant telomere shortening that limits the number of cell divisions in humans [33]. Recent in vitro studies [34] have found that senescence of human primary pancreatic beta cells is responsible for limiting the number of cell divisions. It seems likely that repeated replication during differentiation, such as high cellular turnover during the pathogenesis of liver cirrhosis, could cause islet cells to become senescent. Many studies indicate that the high cellular turnover of beta cells that is caused by beta cell replication and apoptosis is observed in the pathogenesis of type 2 diabetes. However, no previous reports discuss whether beta cell senescence occurs in type 2 diabetes. The current theory is that insufficient beta cell proliferation occurs at an early stage of type 2 diabetes pathogenesis and that the

**Fig. 6** Correlations between cellular senescence and cellular proliferation (a) ( $r=0.864$ ,  $p<0.001$ ) and  $AUC_{\text{glucose}}$  (b) ( $r=0.806$ ,  $p<0.005$ ) of the high-fat diet group and the control group after 12 months. Correlations between cellular senescence and  $AUC_{\text{insulin}}$  (c) ( $r=-0.852$ ,  $p<0.01$ ), insulinogenic index (d) ( $r=-0.857$ ,  $p<0.05$ ), and phospho-p38-positive beta cells (e) ( $r=0.843$ ,  $p<0.05$ ) of the high-fat diet group after 12 months



markedly increased beta cell apoptosis is the main factor of reduced beta cell mass in the pathogenesis of type 2 diabetes. Actually, we observed markedly increased cellular apoptosis after a long-term, high-fat diet. However, in our study (for 4 months) and another [14] longitudinal study in rodents, proliferation of beta cells was found even after a long-term prediabetic stage, suggesting that compensatory beta cell proliferation is maintained until the loss of the remaining beta cell divisions.

In addition to high cellular turnover, there may be another pathway of beta cell senescence in diabetes. Senescence of human primary pancreatic beta cells is caused by a telomere-independent pathway because senescence is not prevented by the expression of telomerase, which extends telomere length [34]. Additionally, telomere length in mice is much longer than in humans, suggesting that telomeres are not related to cellular senescence in mice [35, 36]. Many studies demonstrate that cellular senescence is caused by ROS and is mediated

by enhancing the activity of MAPK, which consists of at least three enzymes, including extracellular signal-regulated kinase (ERK), c-Jun N-terminal kinase (JNK), and p38 MAPK. For example, in rat kidney cells the ageing process parallels increases in ROS that strongly enhance the activities of ERK, JNK, and p38 MAPK [21]. Isawa et al. reported that p38 MAPK is an important causative molecule in both telomere-dependent and telomere-independent cellular senescence, including ROS-induced senescence in both human and mouse fibroblasts [37]. Oxidative stress occurs in the diabetic state [8, 38], and ROS are produced in islets through the non-enzymatic glycosylation reaction and the electron transport chain in mitochondria [12, 39]. It was recently reported that p38 MAPK in isolated rat islets is activated by oxidative stress [40]. In our study, the active form of phospho-p38 was observed in the islets of diet-induced diabetic mice at the late stage of the high-fat diet, but the frequency of phospho-p38 was small compared with the percentage of SA beta-gal staining in the islets. Moreover, there was a significant positive correlation between the frequency of phospho-p38-positive beta cells and the percentage of SA beta-gal-positive area in islets of the high-fat diet group. The cyclin-dependent kinase inhibitors p16 and p21 are increased in p38-activated senescence [37]. Furthermore, oxidative stress induces p21 (WAF1/CIP1/Sdi1) expression in isolated rat islet cells by treatment with H<sub>2</sub>O<sub>2</sub> and pancreatic rat islet cells of hyperglycaemic Zucker diabetic fatty rats [41]. Our results and the previous findings suggest that beta cell senescence is caused by oxidative stress and may be mediated by the p38 MAPK pathway, resulting in the elevation of p21.

In conclusion, decreased beta cell proliferation and cellular senescence are found in diet-induced type 2 diabetic mice. Cellular senescence may be caused by the compensatory rapid proliferation of beta cells needed to maintain adequate beta cell mass and/or the accumulation of ROS in beta cells. Beta cell senescence leads to insufficient insulin release as a consequence of decreased beta cell mass and contributes to the pathogenesis of diet-induced diabetes.

**Acknowledgements** This study was supported by the High-Technology Research Centre Project of Kagawa Nutrition University from the Ministry of Education, Japan. We thank Dr Yasunori Kanazawa (Jichi Medical School Tochigi, Japan) for helpful discussions.

## References

- Poitout V, Robertson RP (2002) Secondary beta-cell failure in type 2 diabetes—a convergence of glucotoxicity and lipotoxicity. *Endocrinology* 143:339–342
- Prentki M, Joly E, El-Assaad W, Roduit R (2002) Malonyl-CoA signalling, lipid partitioning, and glucolipotoxicity: role in beta-cell adaptation and failure in the etiology of diabetes. *Diabetes* 51[Suppl 3]:S405–S413
- Kaiser N, Leibowitz G, Neshler R (2003) Glucotoxicity and beta-cell failure in type 2 diabetes mellitus. *J Pediatr Endocrinol Metab* 16:5–22
- Finegood DT, Scaglia L, Bonner-Weir S (1995) Dynamics of beta-cell mass in the growing rat pancreas. Estimation with a simple mathematical model. *Diabetes* 44:249–256
- Bonner-Weir S (2000) Islet growth and development in the adult. *J Mol Endocrinol* 24:297–302
- Tokuyama Y, Sturis J, DePaoli AM et al (1995) Evolution of beta-cell dysfunction in the male Zucker diabetic fatty rat. *Diabetes* 44:1447–1457
- Corbett J, Serup P, Bonner-Weir S, Nielsen JH (1997) Beta-cell ontogeny: growth and death. *Diabetologia* 40[Suppl 3]:B27–B32
- Sakuraba H, Mizukami H, Yagihashi N, Wada R, Hanyu C, Yagihashi S (2002) Reduced beta-cell mass and expression of oxidative stress-related DNA damage in the islet of Japanese type 2 diabetic patients. *Diabetologia* 45:85–96
- Koyama M, Wada R, Sakuraba H, Mizukami H, Yagihashi S (1998) Accelerated loss of islet beta cells in sucrose-fed Goto-Kakizaki rats, a genetic model of non-insulin-dependent diabetes mellitus. *Am J Pathol* 153:537–545
- Pick A, Clark J, Kubstrup C et al (1998) Role of apoptosis in failure of beta-cell mass compensation for insulin resistance and beta-cell defects in the male Zucker diabetic fatty rat. *Diabetes* 47:358–364
- Donath MY, Gross DJ, Cerasi E, Kaiser N (1999) Hyperglycemia-induced beta-cell apoptosis in pancreatic islets of *Psammomys obesus* during development of diabetes. *Diabetes* 48:738–744
- Kaneto H, Fujii J, Myint T et al (1996) Reducing sugars trigger oxidative modification and apoptosis in pancreatic beta-cells by provoking oxidative stress through the glycation reaction. *Biochem J* 320:855–863
- Ritzel RA, Butler PC (2003) Replication increases beta-cell vulnerability to human islet amyloid polypeptide-induced apoptosis. *Diabetes* 52:1701–1708
- Butler AE, Janson J, Soeller WC, Butler PC (2003) Increased beta-cell apoptosis prevents adaptive increase in beta-cell mass in mouse model of type 2 diabetes: evidence for role of islet amyloid formation rather than direct action of amyloid. *Diabetes* 52:2304–2314
- Maedler K, Spinas GA, Lehmann R et al (2001) Glucose induces beta-cell apoptosis via upregulation of the Fas receptor in human islets. *Diabetes* 50:1683–1690
- Maedler K, Fontana A, Ris F et al (2002) FLIP switches Fas-mediated glucose signalling in human pancreatic beta cells from apoptosis to cell replication. *Proc Natl Acad Sci U S A* 99:8236–8241
- Maedler K, Sergeev P, Ris F et al (2002) Glucose-induced beta cell production of IL-1beta contributes to glucotoxicity in human pancreatic islets. *J Clin Invest* 110:851–860
- Federici M, Hribal M, Perego L et al (2001) High glucose causes apoptosis in cultured human pancreatic islets of Langerhans: a potential role for regulation of specific Bcl family genes toward an apoptotic cell death program. *Diabetes* 50:1290–1301
- Hayflick L, Moorhead PS (1961) The serial cultivation of human diploid cell strains. *Exp Cell Res* 25:585–621
- Martin GM, Austad SN, Johnson TE (1996) Genetic analysis of ageing: role of oxidative damage and environmental stresses. *Nat Genet* 13:25–34
- Chen Q, Ames BN (1994) Senescence-like growth arrest induced by hydrogen peroxide in human diploid fibroblast F65 cells. *Proc Natl Acad Sci U S A* 91:4130–4134
- Kim HJ, Jung KJ, Yu BP, Cho CG, Chung HY (2002) Influence of aging and calorie restriction on MAPKs activity in rat kidney. *Exp Gerontol* 37:1041–1053
- Hutter E, Unterluggauer H, Uberall F, Schramek H, Jansen-Durr P (2002) Replicative senescence of human fibroblasts: the role of Ras-dependent signaling and oxidative stress. *Exp Gerontol* 37:1165–1174
- Ihara Y, Toyokuni S, Uchida K et al (1999) Hyperglycaemia causes oxidative stress in pancreatic beta-cells of GK rats, a model of type 2 diabetes. *Diabetes* 48:927–932

25. Surwit RS, Kuhn CM, Cochrane C, McCubbin JA, Feinglos MN (1988) Diet-induced type 2 diabetes in C57BL/6J mice. *Diabetes* 37:1163–1167
26. Surwit RS, Feinglos MN, Rodin J et al (1995) Differential effects of fat and sucrose on the development of obesity and diabetes in C57BL/6J and A/J mice. *Metabolism* 44:645–651
27. Reeves PG, Nielsen FH, Fahey GC Jr (1993) AIN-93 purified diets for laboratory rodents: final report of the American Institute of Nutrition ad hoc writing committee on the reformulation of the AIN-76A rodent diet. *J Nutr* 123:1939–1951
28. Okamoto H (1981) Regulation of proinsulin synthesis in pancreatic islets and a new aspect to insulin-dependent diabetes. *Mol Cell Biochem* 37:43–61
29. Sone H, Sasaki Y, Komai M, Toyomizu M, Kagawa Y, Furukawa Y (2004) Biotin enhances ATP synthesis in pancreatic islets of the rat, resulting in reinforcement of glucose-induced insulin secretion. *Biochem Biophys Res Commun* 314:824–829
30. Kido Y, Burks DJ, Withers D et al (2000) Tissue-specific insulin resistance in mice with mutations in the insulin receptor, IRS-1, and IRS-2. *J Clin Invest* 105:199–205
31. Butler AE, Janson J, Bonner-Weir S, Ritzel R, Rizza RA, Butler PC (2003) Beta-cell deficit and increased beta-cell apoptosis in humans with type 2 diabetes. *Diabetes* 52:102–110
32. Buckner FS, Wilson AJ, Van Voorhis WC (1999) Detection of live *Trypanosoma cruzi* in tissues of infected mice by using histochemical stain for beta-galactosidase. *Infect Immun* 67:403–409
33. Rudolph KL, Chang S, Millard M, Schreiber-Agus N, DePinho RA (2000) Inhibition of experimental liver cirrhosis in mice by telomerase gene delivery. *Science* 287:1253–1258
34. Halvorsen TL, Beattie GM, Lopez AD, Hayek A, Levine F (2000) Accelerated telomere shortening and senescence in human pancreatic islet cells stimulated to divide in vitro. *J Endocrinol* 166:103–109
35. Kipling D, Cooke HJ (1990) Hypervariable ultra-long telomeres in mice. *Nature* 347:400–402
36. Manning EL, Crossland J, Dewey MJ, Van Zant G (2002) Influences of inbreeding and genetics on telomere length in mice. *Mamm Genome* 13:234–238
37. Iwasa H, Han J, Ishikawa F (2003) Mitogen-activated protein kinase p38 defines the common senescence-signalling pathway. *Genes Cells* 8:131–144.
38. Nishikawa T, Edelstein D, Du XL et al (2000) Normalizing mitochondrial superoxide production blocks three pathways of hyperglycaemic damage. *Nature* 404:787–790
39. Tiedge M, Lortz S, Drinkgern J, Lenzen S (1997) Relation between antioxidant enzyme gene expression and antioxidative defense status of insulin-producing cells. *Diabetes* 46:1733–1742
40. Kaneto H, Xu G, Fujii N, Kim S, Bonner-Weir S, Weir GC (2002) Involvement of c-Jun N-terminal kinase in oxidative stress-mediated suppression of insulin gene expression. *J Biol Chem* 277:30010–30018
41. Kaneto H, Kajimoto Y, Fujitani Y et al (1999) Oxidative stress induces p21 expression in pancreatic islet cells: possible implication in beta cell dysfunction. *Diabetologia* 42:1093–1097